Supporting Information

Rational Synthesis of Novel "Giant" CuInTeSe/CdS Core/Shell Quantum Dots for Optoelectronics

Jing-Yin Xu[a], Xin Tong[*a,b], Lucas V. Besteiro[a,e], Xin Li[a], Chenxia Hu[c], Ruitong Liu[c], Ali Imran Channa[a], Haiguang Zhao[d], Federico Rosei[a,e], Alexander O. Govorov[f], Qiang Wang[*c] and Zhiming M. Wang[*a,b,g]

[a] Institute of Fundamental and Frontier Sciences, University of Electronic Science and Technology of China, Chengdu 610054, P. R. China.

[b] Yangtze Delta Region Institute (Huzhou), University of Electronic Science and Technology of China, Huzhou 313001, P. R. China.

[c] State Key Laboratory of Applied Organic Chemistry, Key Laboratory of Special Function Materials and Structure Design, College of Chemistry and Chemical Engineering, Lanzhou University, Lanzhou 730000, P. R. China.

[d] College of Physics & State Key Laboratory of Bio-Fibers and Eco-Textiles, Qingdao University, No. 308 Ningxia Road, Qingdao 266071 P. R. China.

[e] Institut National de la Recherche Scientifique, Centre Énergie, Matériaux et Télécommunications, 1650 Boul. Lionel Boulet, J3X 1S2 Varennes, Québec, Canada.

[f] Department of Physics and Astronomy, Ohio University, Athens OH 45701, USA.

[g] Institute of Microengineering and Nanoelectronics (IMEN), Universiti Kebangsaan Malaysia, 43600, Bangi, Selangor, Malaysia.

[*]Corresponding authors: xin.tong@uestc.edu.cn, qiangwang@lzu.edu.cn, zhmwang@uestc.edu.cn

Table S1. Sizes of QDs with different injection volumes of precursors.

Sample Labels	S0	S1	S2	S3	S4	S5
Injection Volume (mL)	0	1	2	3	4	5
Size (nm)	2±0.5	3±1	4±0.5	7±0.8	8.5±1	9.5±1.2

Table S2. Lattice distance of S0-S5 QDs.

Samples	2θ	crystal plane	d_{XRD}(Å)	d_{TEM} (nm)
S0	25.5	(112)	3.46	0.34
S1	25.8	(111)	3.44	0.35
S2	26.1	(111)	3.40	0.34
S3	26.2	(111)	3.39	0.34
S4	26.4	(111)	3.37	0.33
S5	26.5	(111)	3.36	0.33

Interplanar distance calculations: The lattice parameters of QDs were calculated based on the following equations：

$$n\lambda = 2dsin\theta \quad (1)$$

Where the n is first-order diffraction and λ is the diffracted wavelengths (Cu Kα radiation). The θ is the Bragg's angle. *d* is the lattice spacing.

Table S3. The PL emission peaks and corresponding average PL lifetime of g-QDs with diverse shell thicknesses.

Sample Labels	S1	S2	S3	S4	S5
PL Peaks (nm)	~915	~970	~1080	~1095	~1200
PL Lifetime (μs)	10.5	11.9	12.2	12.4	14.0
PL Quantum Yields	4.6%	7.3%	5.4%	2.4%	1.8%

Table S4. PL emission and lifetime of core/shell g-QDs with respect to as-synthesized pyramidal shaped g-QDs.

QDs type	PL emission (nm)	PL lifetime (ns)	Reference
CdSe/CdS	~650 nm	~40	[1]
CISeS/CdSeS/CdS	~830	~2000	[2]
PbSe/CdSe/CdSe	~1400	~2000	[3]
$CuInSe_2/CuInS_2$	~1100	~300	[4]
InP/CdSe	~1000	~300	[5]
CuInTeSe/CdS	~1200	~14000	This work

Table S5. Fitting results of lifetime components for S0 and S4 g-QDs at different probe wavelength with 900 nm, 1000 nm, 1100 nm and 1200 nm.

Wavelength(nm)	Sample Labels	τ_1	τ_2	τ_3
900	**S0**	426.2 fs (87%)	11.8 ps (-10%)	267.9 ps (-3%)
900	**S4**	530.8 fs (84%)	43.6 ps (-9%)	250.9 ps (-7%)
1000	**S0**	718.1 ps (76%)	3.4 ps (18%)	73 ps (6%)
1000	**S4**	266.0 fs (71%)	3.1 ps (24%)	105.6 ps (5%)
1100	**S0**	987.3 fs (66%)	5.4 ps (23%)	81.5 ps (11%)
1100	**S4**	2.2 ps (47%)	36.8 ps (14%)	>ns (39%)
1200	**S0**	1.1 ps (62%)	5.9 ps (25%)	80.1 ps (13%)
1200	**S4**	2.4 ps (37%)	34.4 ps (10%)	>ns (53%)

Table S6. The geometrical parameters of QDs used in theoretical modeling.

Size (nm)	S0	S1	S2	S3	S4	S5
CuInTeSe core	2	2	2	2	2	2
CdS shell	-	1	2	5	6.5	7.5
Total size	2	3	4	7	8.5	9.5
Number of impurities In_{Cu} (Cu:In=1:1)	2	2	2	2	2	2

Table S7. Physical parameters used in theoretical modeling.[6-9]

	E_v (eV)	E_c (eV)	E_g (eV)	m_e/m_0	m_{hh}/m_0
CuInTeSe	-5.97	-4.57	1.40	0.09	0.71
CdS	-6.45	-4.2	2.25	0.18	0.53
Vacuum level	-9.8	0	-	1	-

Table S8. Performance comparison of recent g-QDs-based PEC systems.

QDs type	PEC performance (mA/cm^2)	Reference
$CdSe_xTe_{1-x}$@CdS	3	[10]
PbS/CdS	5.3	[11]
$CuInSe_xS_{2-x}$/CdSeS/CdS	5.5	[2]
$CuInSe_2/CuInS_2$	3.1	[4]
CuInTeSe/CdS	4.5	This work

Table S9. The photocurrent densities of QDs-based PEC devices.

Sample Labels	**S0**	**S1**	**S2**	**S3**	**S4**	**S5**
Photocurrent densities (mA/cm^2)	0.8(±0.1)	1.3(±0.2)	1.4(±0.1)	3.5(±0.2)	4.5(±0.3)	3.1(±0.3)

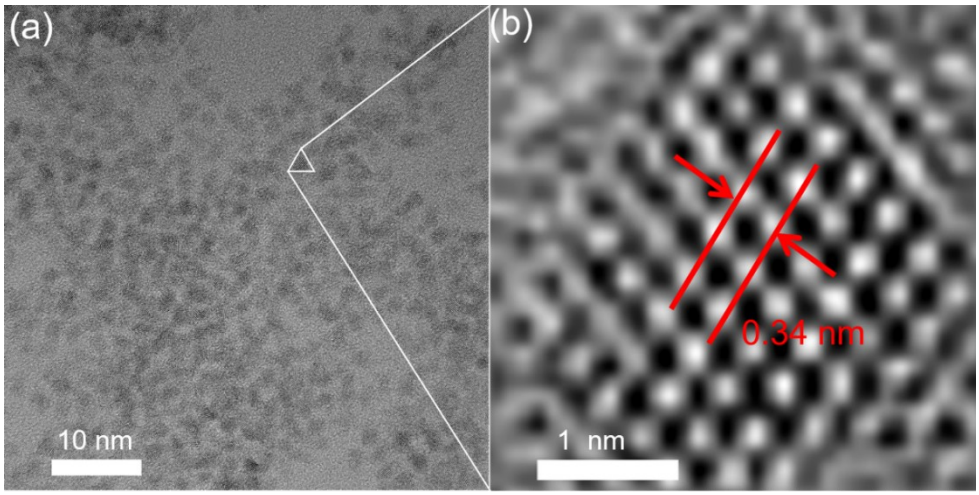

Figure S1. (a) TEM and (b) HRTEM images of S0 core QDs.

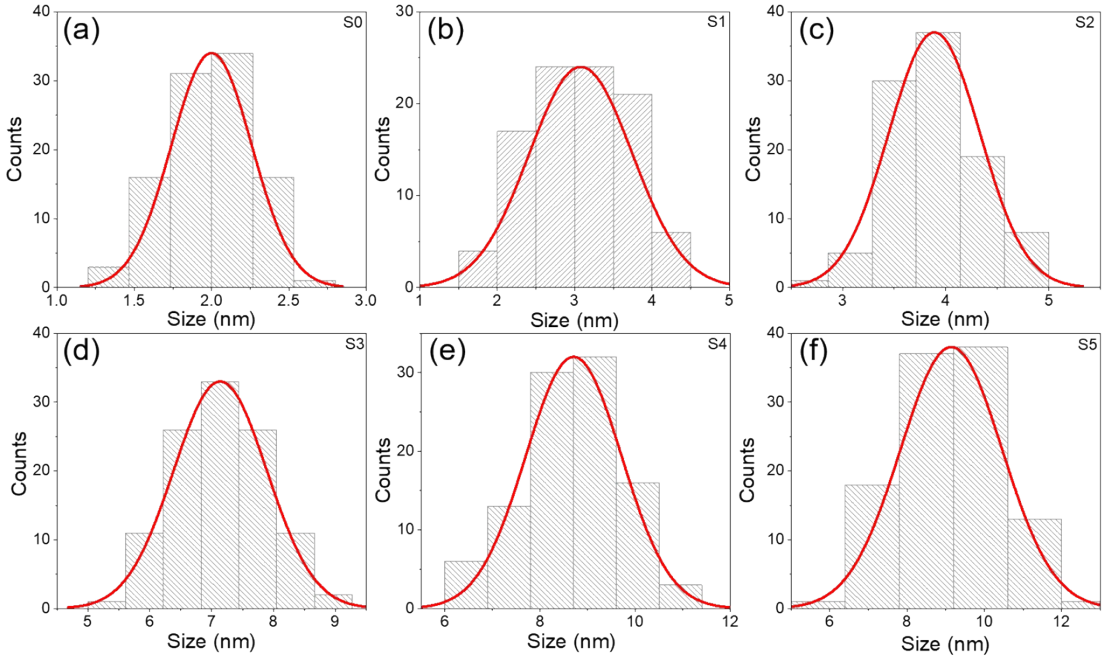

Figure S2. Size ditribution of S0-S5 QDs.

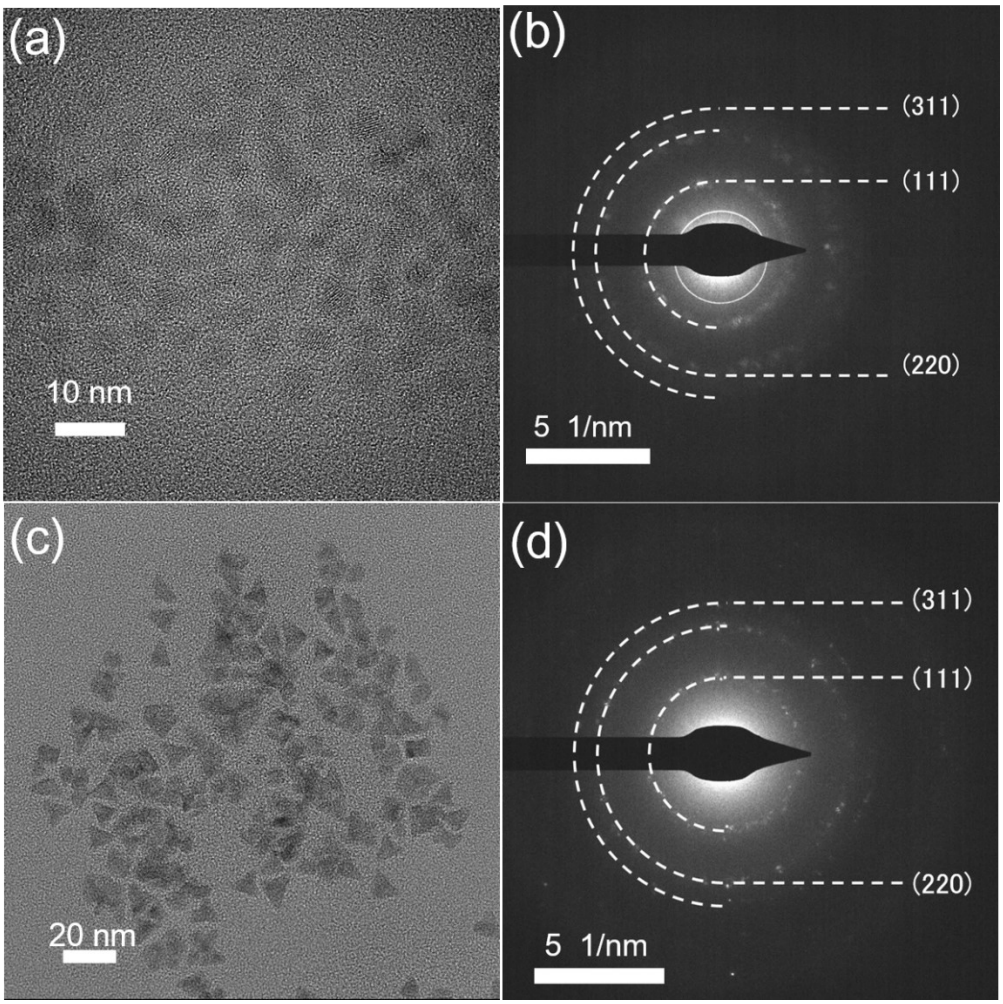

Figure S3. (a) TEM images and (b) SAED pattern of S1 QDs; (c) TEM images and (d) SAED pattern of S5 g-QDs.

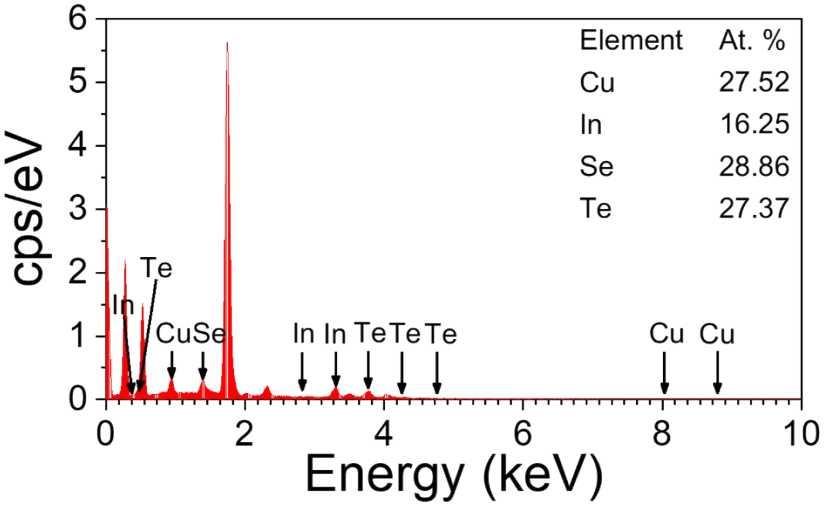

Figure S4. EDS spectrum of CITS QDs. The spectrum confirms all the elements including Cu, In, Se and Te in core QDs.

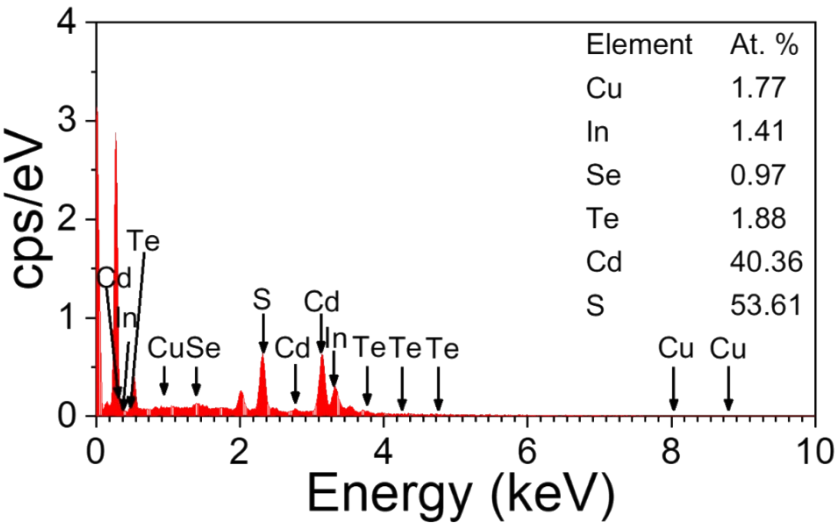

Figure S5. EDS spectrum of CITS/CdS core/shell QDs. The spectrum confirms all the elements including Cu, In, Se, Te, Cd and S in the core/shell QDs.

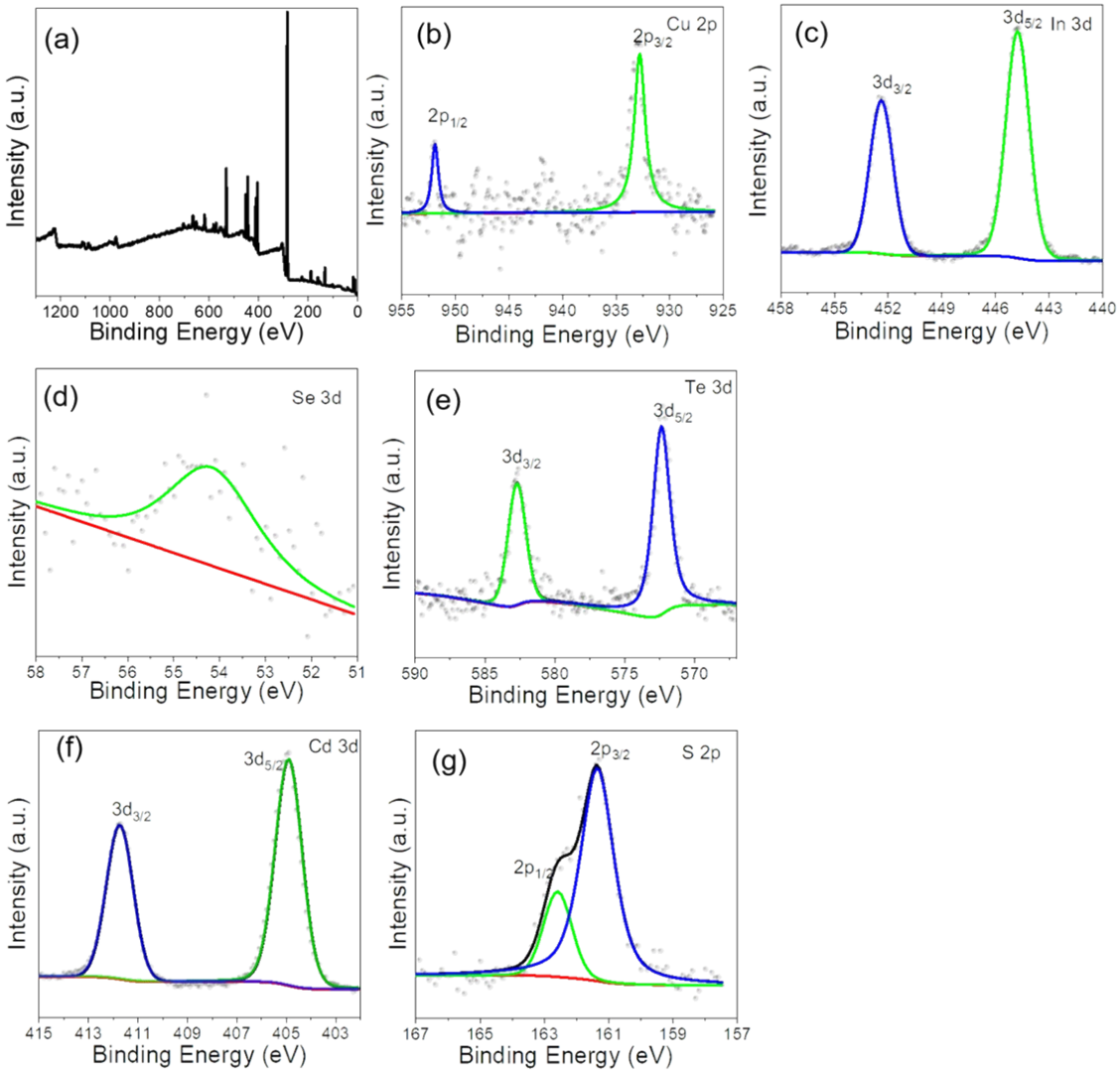

Figure S6. (a) XPS survey spectra and (b)-(g) HRXPS spectra for Cu 2p, In 3d, Se 3d, Te 3d, Cd 3d and S 2p core levels in CITS/CdS core/shell QDs, respectively.

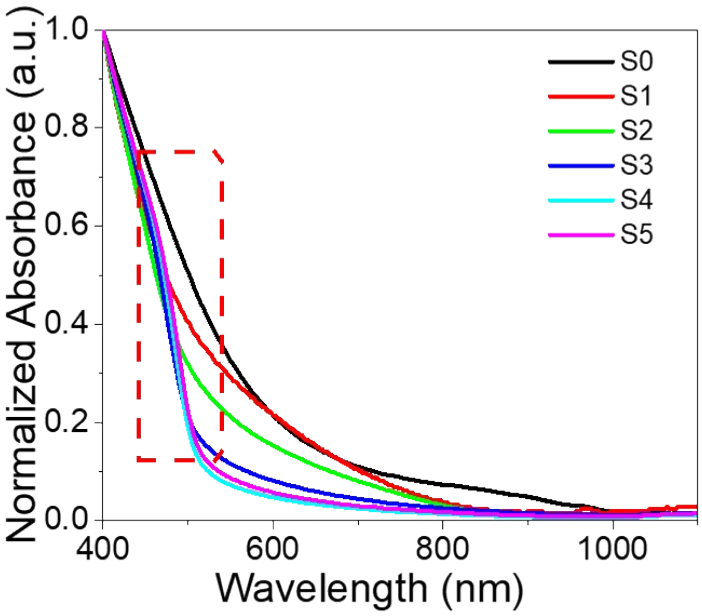

Figure S7. Normalized absorption spectra of QDs at 400 nm with exciton peaks labeled by the red dashed box.

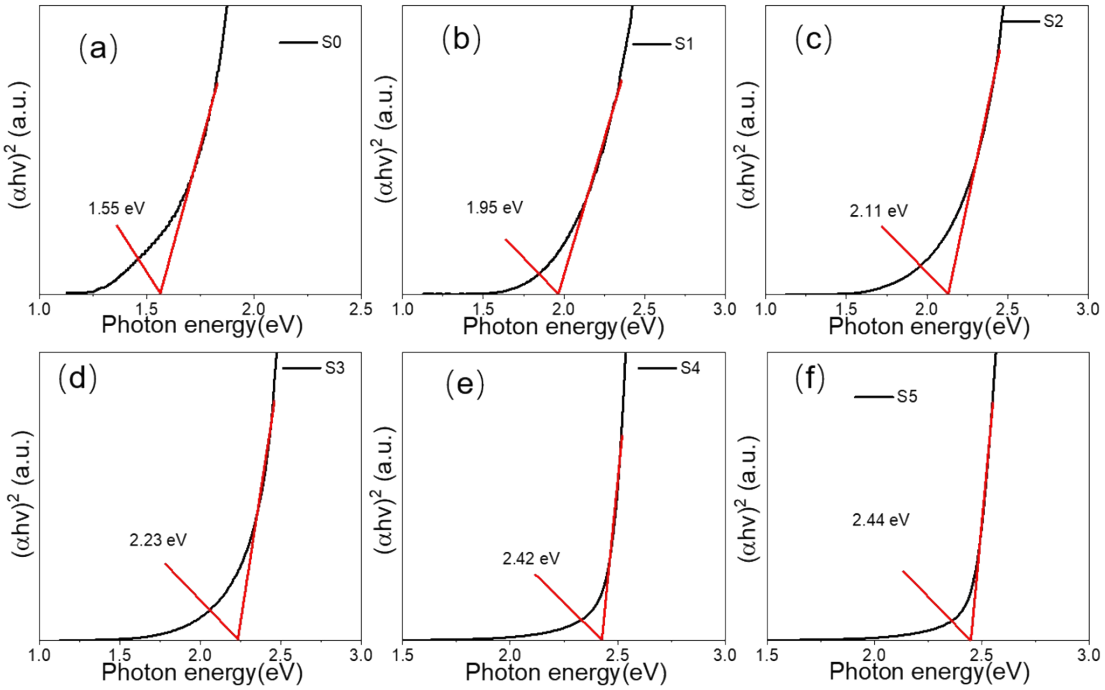

Figure S8. Tauc plot derived from absorption spectra of S0-S5 QDs.

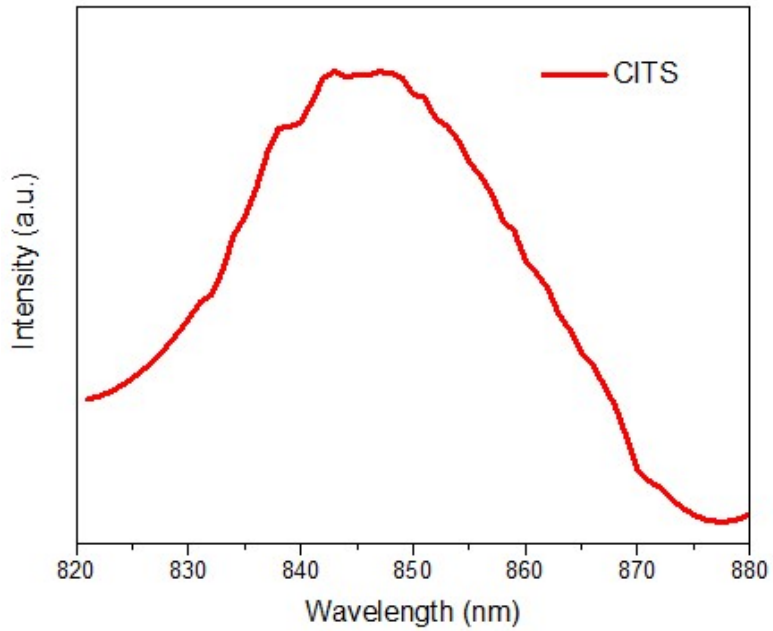

Figure S9. PL emission spectra of CITS core QDs.

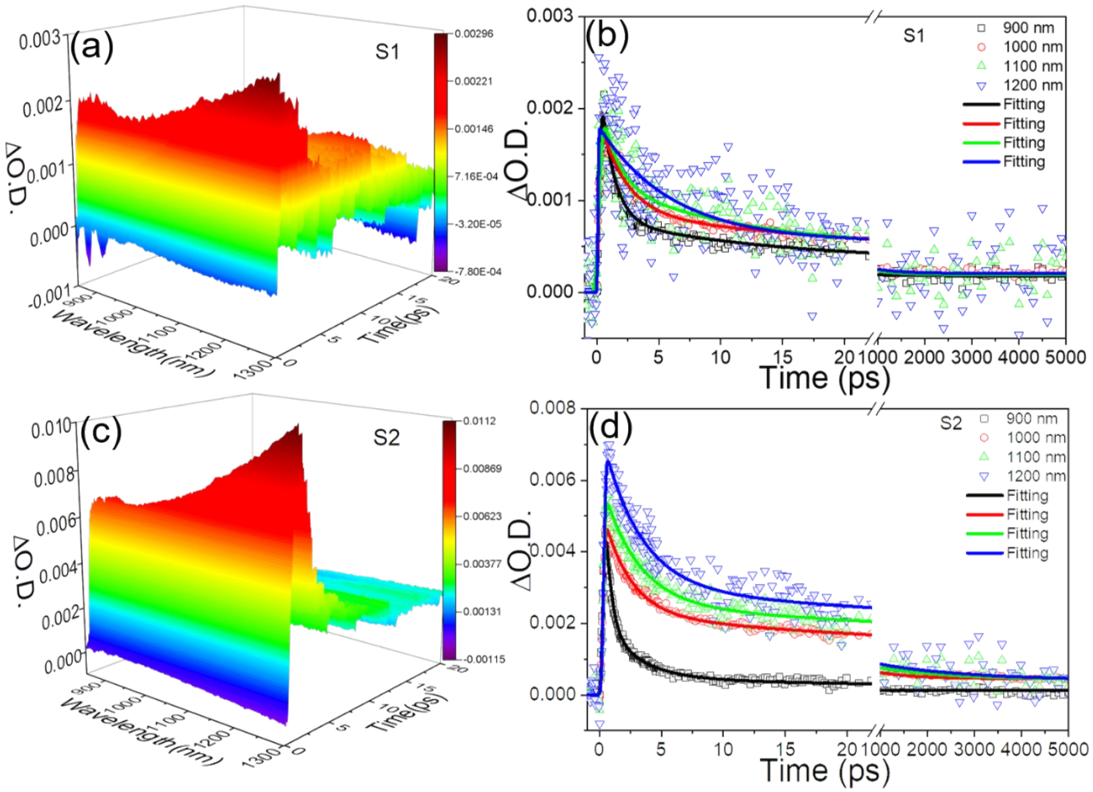

Figure S10. (a) 3D transient time delay-wavelength-delta optical density mapping of S1 QDs in the NIR region (pump wavelength: 500 nm). (b) Time decay curves probed at 900, 1000, 1100 and 1200 nm; (c) The 3D plot of TA spectra of S2 QDs upon 500 nm excitation. (d) Representative decay curves recorded at 900, 1000, 1100 and 1200 nm.

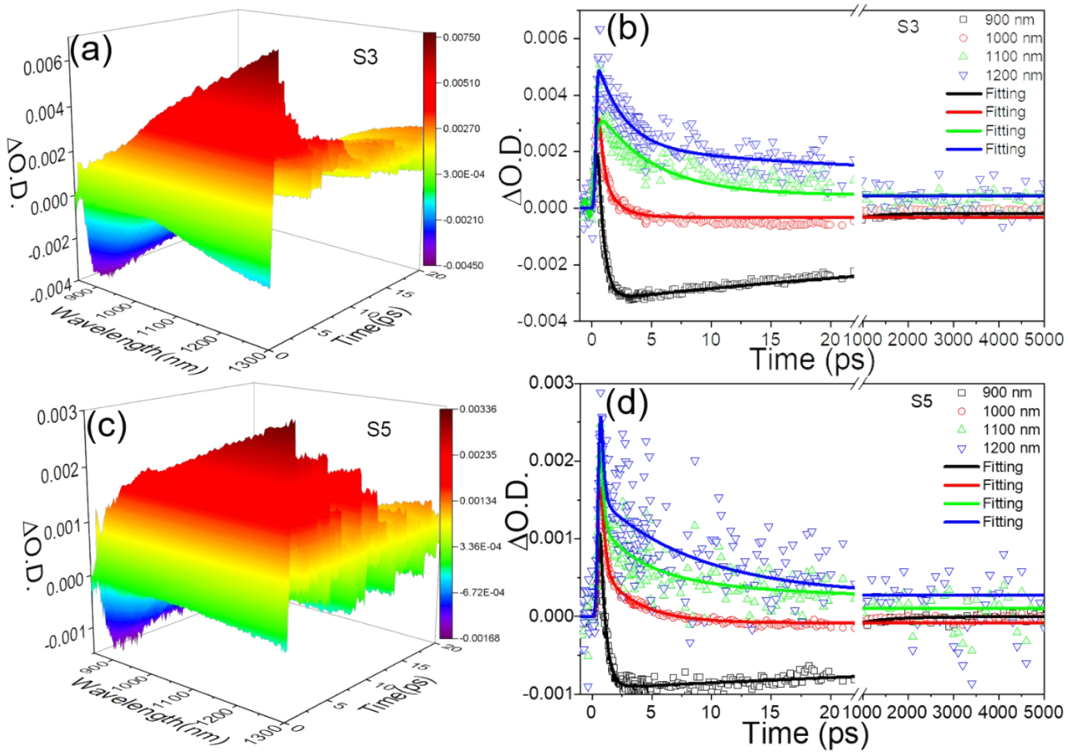

Figure S11. (a) TA spectra of S3 g-QDs in toluene. (b) Typical decay curves recorded at 900, 1000, 1100 and 1200 nm; TA spectra of S5 g-QDs: (c) the 3D plot, (d) time delay profiles recorded at 900, 1000, 1100 and 1200 nm.

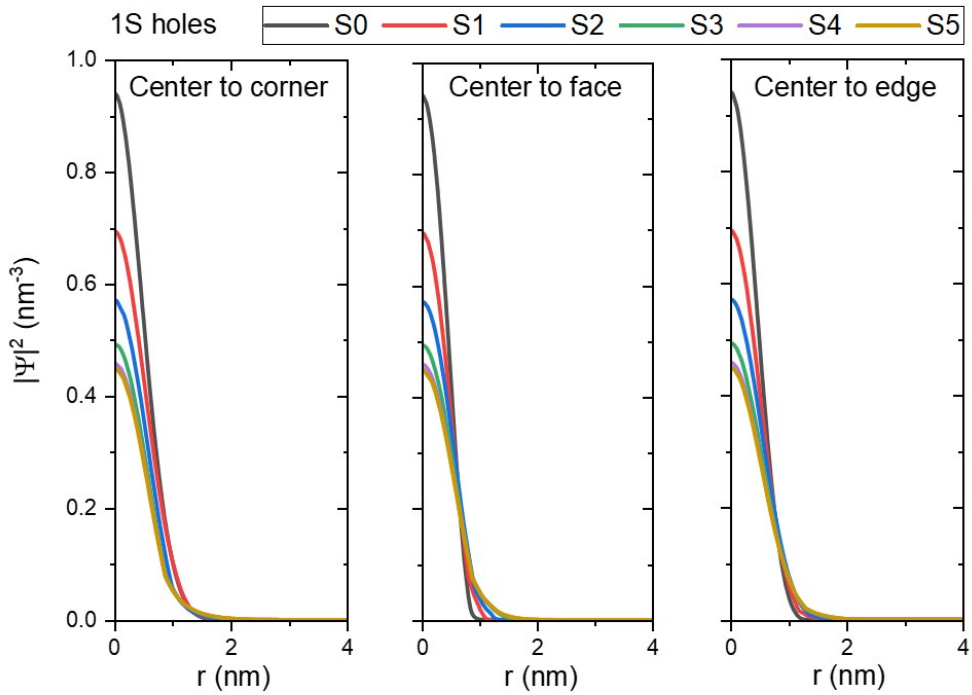

Figure S12. Spatial extension of the highest energy holes, obtained with the method described in the main text. It is clear that the holes remain mostly localized at the core of the heterogeneous QDs and do not become as delocalized as the electrons.

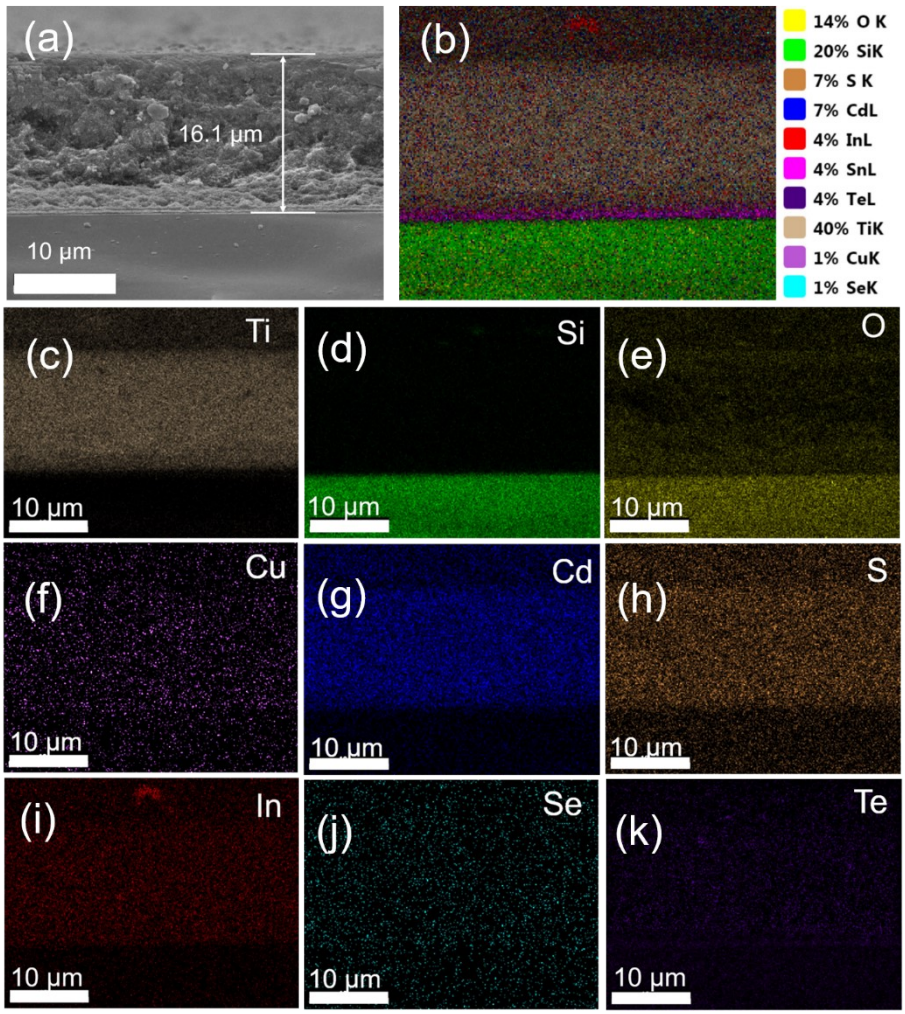

Figure S13. (a) Cross-sectional SEM image of CITS/CdS g-QDs-sensitized photoanode and corresponding EDS mapping analysis of (c) Ti, (d) Si, (e) O, (f) Cu, (g) Cd, (h) S, (i) In, (j) Se and (k) Te.

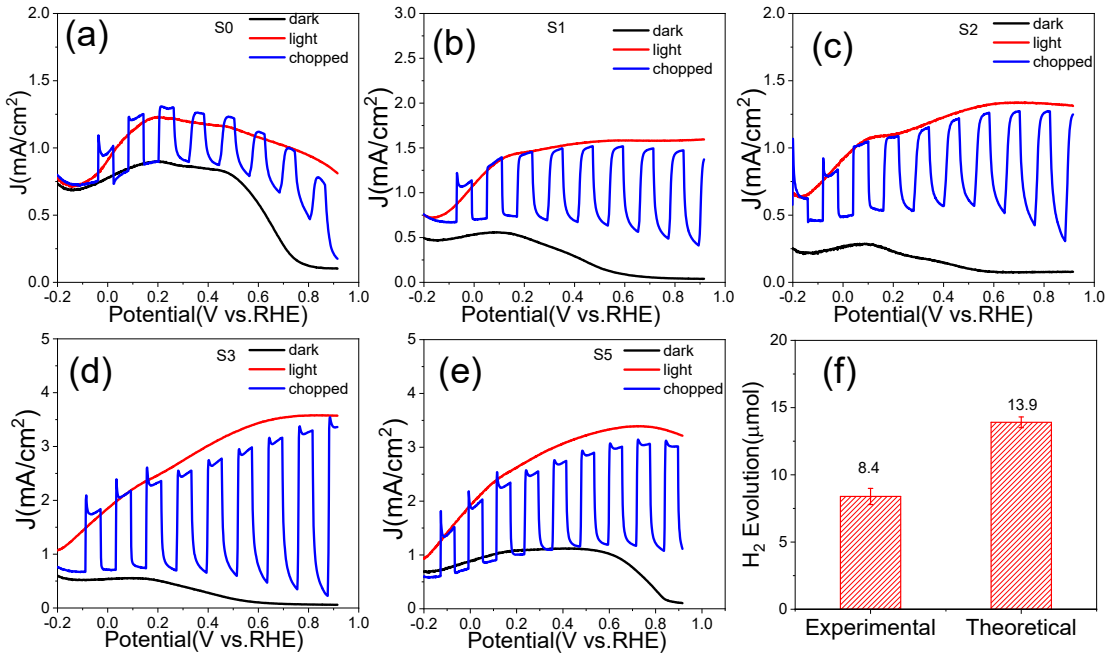

Figure S14. Photocurrent density versus the potential of RHE for the CITS core (a), S1(b), S2(c), S3(d), S5(e) QDs-based photoanode in dark, under continuous and chopped light illumination (AM 1.5G, 100 mW/cm^2). (f) Hydrogen production of the S4 g-QDs-based PEC cell in 7200s.

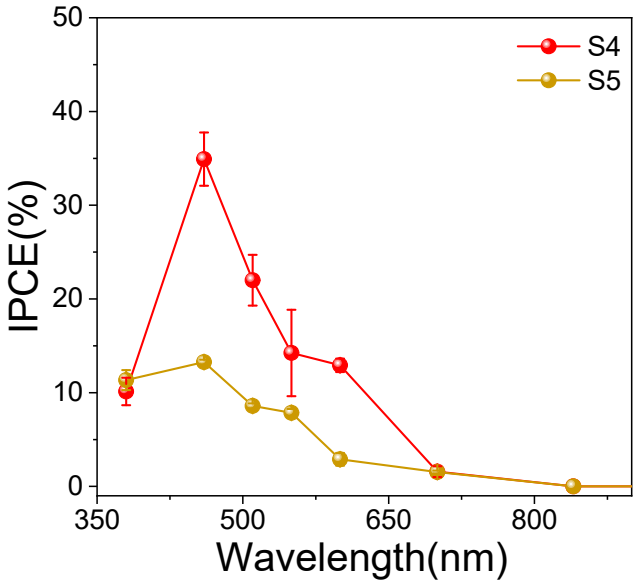

Figure S15. Comparison of IPCE spectra for S4 and S5 QDs-based PEC devices.

References

1. G. S. Selopal, H. Zhao, X. Tong, D. Benetti, F. Navarro-Pardo, Y. Zhou, D. Barba, F. Vidal, Z. M. Wang and F. Rosei, *Adv. Funct. Mater.*, 2017, **27**, 1701468.
2. X. Tong, X. T. Kong, C. Wang, Y. Zhou, F. Navarro-Pardo, D. Barba, D. Ma, S. Sun, A. O. Govorov, H. Zhao, Z. M. Wang and F. Rosei, *Adv. Sci.*, 2018, **5**, 1800656.
3. C. J. Hanson, N. F. Hartmann, A. Singh, X. Ma, W. J. I. DeBenedetti, J. L. Casson, J. K. Grey, Y. J. Chabal, A. V. Malko, M. Sykora, A. Piryatinski, H. Htoon and J. A. Hollingsworth, *J. Am. Chem. Soc.*, 2017, **139**, 11081-11088.
4. X. Tong, X.-T. Kong, Y. Zhou, F. Navarro-Pardo, G. S. Selopal, S. Sun, A. O. Govorov, H. Zhao, Z. M. Wang and F. Rosei, *Adv. Energy Mater.*, 2018, **8**, 1701432.
5. A. M. Dennis, M. R. Buck, F. Wang, N. F. Hartmann, S. Majumder, J. L. Casson, J. D. Watt, S. K. Doorn, H. Htoon, M. Sykora and J. A. Hollingsworth, *Adv. Funct. Mater.*, 2019, **29**, 1809111.
6. H. Neumann, *Solar Cells*, 1986, **16**, 317-333.
7. S. B. Zhang, S.-H. Wei, A. Zunger and H. Katayama-Yoshida, *Phys. Rev. B*, 1998, **57**, 9642-9656.
8. P. E. Lippens and M. Lannoo, *Phys. Rev. B*, 1989, **39**, 10935-10942.
9. M. Gratzel, *Nature*, 2001, **414**, 338-344.
10. G. J. Liu, Z. B. Ling, Y. Q. Wang and H. G. Zhao, *Int. J. Hydrogen Energy*, 2018, **43**, 22064-22074.
11. L. Jin, G. Sirigu, X. Tong, A. Camellini, A. Parisini, G. Nicotra, C. Spinella, H. G. Zhao, S. H. Sun, V. Morandi, M. Zavelani-Rossi, F. Rosei and A. Vomiero, *Nano Energy*, 2016, **30**, 531-541.